

Measurement of cellular forces at focal adhesions using elastic micro-patterned substrates

U.S. Schwarz^{a,b,*}, N.Q. Balaban^{c,d}, D. Riveline^{d,e}, L. Addadi^f, A. Bershadsky^d,
S.A. Safran^b, B. Geiger^d

^aTheory Division, Max-Planck-Institute of Colloids and Interfaces, Potsdam 14467, Germany

^bDepartment of Materials and Interfaces, The Weizmann Institute of Science, Rehovot 76100, Israel

^cLaboratory of Living Matter, Rockefeller University, New York, NY 10021, USA

^dDepartment of Molecular Cell Biology, The Weizmann Institute of Science, Rehovot 76100, Israel

^eLaboratoire de Spectrométrie Physique, UMR 5588, Université Joseph Fourier-CNRS, BP 87, 38402 Saint-Martin-d'Hères Cedex, France

^fDepartment of Structural Biology, The Weizmann Institute of Science, Rehovot 76100, Israel

Abstract

Mechanical force is known to play an important role in the regulation of cellular behaviour, including adhesion, motility, differentiation and proliferation. For stationary, mechanically active cells like fibroblasts, adhesion to flat substrates occurs mainly at sites of focal adhesions, which are micron-sized protein aggregates at the plasma membrane, which on the cytoplasmic side connect to the actin cytoskeleton. In recent years, evidence has been growing that focal adhesions act as mechanosensors which convert mechanical force into biochemical signalling. We have investigated the relationship between force and aggregation at focal adhesions by a new method which combines elastic micro-patterned substrates (to record substrate deformation), fluorescence labelling of focal adhesion proteins (to monitor aggregation) and numerical solution of the inverse problem of linear elasticity theory (to calculate forces at focal adhesions). We have found that force correlates linearly with lateral size of aggregation, with a stress constant of $5.5 \text{ nN}/\mu\text{m}^2$. This finding indicates that mechanosensing involves regulation of aggregation.

© 2002 Elsevier Science B.V. All rights reserved.

Keywords: Cell–matrix adhesion; Focal adhesions; Integrins; Mechanosensor; Elasticity theory; Inverse problems

1. Introduction

Cells are highly complex machines which permanently have to make important decisions by integrating all available information about their environment [1]. In aqueous solution, cell communication with the environment is essentially restricted to biochemical channels. However, when cells start to contact extracellular structures, physical information like the elastic properties of the environment become available and can be integrated into cellular decision making. In a biological context, contact might be achieved with other cells or the extracellular matrix. In a technological context, contact might be achieved with synthetic material like glass, plastic, metal or semiconductor surfaces. In all of

these cases, physical contact with the environment opens up the possibility of forces developing at the interface between the cell and its environment. These forces can be either external (e.g. shear forces in blood flow) or internal (strong forces in animal cells usually result from the actin part of the cytoskeleton). It is well known that forces do indeed feed directly into cellular regulation [2–4]. One prominent example is bone cells, which are known to become inactive when mechanical input is lacking (e.g. during times of hospitalisation). Mechanical effects are also known for epithelial cells during angiogenesis [5], for fibroblasts during tissue maintenance and wound contraction [6,7], and for locomoting cells in general, e.g. during development, inflammation and metastasis. Recently, a direct connection between application of external force and cytoskeletal and biochemical responses has been demonstrated for single cells in culture [8,9].

When cultured on flat substrates, animal cells develop different kinds of adhesion sites, which can be classified

* Corresponding author. Theory Division, Max-Planck-Institute of Colloids and Interfaces, Potsdam 14467, Germany.

E-mail address: Ulrich.Schwarz@mpikg-golm.mpg.de (U.S. Schwarz).

according to their composition and morphology [10]. The molecular basis for cell–matrix adhesions are the adhesion molecules from the integrin family [11]. Integrins are heterodimers with one of eighteen α and one of eight β subunits. They bind to proteins from the extracellular matrix (e.g. fibronectin, vitronectin, laminin and collagen) mainly through the amino acid sequence Arg–Gly–Asp (RGD motive). Upon extracellular binding, integrin clusters and induce build-up of a cytoplasmic plaque, which in turn connects to the actin cytoskeleton. The most prominent type of cell–matrix adhesion are focal adhesions (FAs), which are elongated protein aggregation clusters associated with the ends of actin filament bundles. FAs typically occur in mature adhesion situations on flat substrates and their cytoplasmic plaque can be very large, involving more than 50 different types of proteins. Traditionally, FAs have been identified as dark areas in interference reflection microscopy [12], and as regions of close approach in transmission electron microscopy [13]. They can also be identified by using immunostaining or fluorescence-constructs for its molecular constituents. In recent years, constructs with green fluorescent protein (GFP) have been used, for e.g. integrin, vinculin, paxillin or zyxin. Due to their large signalling activity, FAs can also be immunostained with antibodies to phosphotyrosine. Although it has been pointed out recently that physiological adhesions in a three-dimensional collagen gel somehow differ in composition and morphology from classical FAs developed on flat substrates [14], FAs provide an excellent model system for integrin-mediated crosstalk between cell and matrix. Moreover, similar structures are indeed formed in certain physiological situations, e.g. by myofibroblasts during wound contraction.

If one is interested in the mechanical information transmitted during cell adhesion, an experimental method has to be developed to measure cellular forces. Since the pioneering work of Harris et al. [15,16] in the early 1980s, the method of choice are elastic substrates (for recent reviews, see Refs. [17,18]). Harris et al. started with thin films of heat polymerised silicone fluids. Polydimethylsiloxane (PDMS) is ideal for microscopic investigation of cells, as it is transparent and nontoxic. Recent improvements of this method include the use of UV light for finer tuning of the surface rigidity [19]. When cells plated on these thin polymers films become mechanically active, the substrate wrinkles in a way which is characteristic for the force pattern applied and which is easy to detect in the microscope. However, since buckling of thin films is an essentially unsolved problem in elasticity theory [20], quantitative analysis of wrinkling assays is hardly possible. The first step towards quantitative analysis, therefore, consisted of suppressing wrinkling by prestress, that is, by fixing the polymer film at the sides [21]. Insertion of marker beads into the polymer film allows the monitoring of substrate deformation under cell traction. In order to quantitatively derive cellular force patterns from this kind of deformation data, one has to use linear elasticity theory of thin films and standard methods to solve inverse

problems (because elasticity theory describes how displacement follows from force, see below) [22]. This computational method was developed by Dembo et al. [23,24], and first applied to locomotion of keratocytes. Keratocytes are fan-shaped, fast moving cells from fish epidermis, and the surprising outcome of these experiments was that the major tractions are exerted as a pinching force pair from the wings of the cell, that is perpendicular to the direction of cell locomotion.

Keratocytes are relatively weak cells, and the main model for mechanical active animal cells, the fibroblast, is too strong as to be used on thin polymer films. Quantitative studies of fibroblast traction became possible by using thick polymer films which, in fact, do not require any prestress to prevent wrinkling. Pelham and Wang [25] introduced the use of thick films of polyacrylamide gels. The use of marker beads embedded in the polymer films again allows the measuring of substrate deformation. For typical film thickness of 70 μm and Young modulus in the order of kilopascals, typical displacements under fibroblast traction are in the order of few microns. Since this is much smaller than film thickness, the polymer substrate can be described as elastic halfspace, whose elasticity theory is well known (Boussinesq problem, see Ref. [20]). Dembo et al. [26,27] again used standard methods for inverse problems to quantitatively analyse fibroblast traction during locomotion. The main results of these studies are that fibroblasts traction is mainly directed from the leading and trailing edges towards the cell center, that cell locomotion and state of FAs depend on substrate elasticity, and that cells are guided by elasticity gradients (they prefer regions of stiffer elasticity). Recently, this method has been combined with the use of GFP-zyxin (one of the proteins localizing to FAs) [28]. The surprising result of this study is that small nascent adhesion complexes near the leading edge correspond to larger forces than the more mature FAs closer to the cell body.

In the work described until now, cellular force patterns were reconstructed as continuous force fields emanating from underneath the cell body. The advantage of this method is that it makes no assumptions about the distribution of forces. However, this approach does not allow quantitative statements on single FAs. Recently, we developed a new method that allowed, for the first time, to measure cellular forces at the level of FAs [29,30]. We used thick PDMS films (typical film thickness, 40 μm ; typical Young modulus, 10 kPa), whose surface was micro-patterned in order to provide a convenient coordinate system on the substrate surface. With a shallow surface pattern, contact guidance through topographic features can be avoided. Then, the use of micro-patterned surfaces offers an attractive alternative to the use of marker beads, since it allows for homogeneous and convenient tracking of substrate deformations. Deformations of the regular pattern are readily seen, without the need to compare between different frames. The use of a GFP-construct for vinculin (a major component of the cytoplasmic plaque of FAs) allows the determination

of the position of the FAs. Assuming that for stationary fibroblasts in mature adhesion, FAs are the main sites for force transmission to the elastic substrate, we used linear elasticity theory and methods for inverse problems to reconstruct single forces at FAs and to correlate them with the size of FAs. The main result of this study is that for stationary fibroblasts, typical forces at mature FAs are between 10 and 30 nN and that there is a linear relationship between force and size of FAs, with a stress constant of $5.5 \text{ nN}/\mu\text{m}^2$.

In this contribution, we will describe our new method in more detail, present our main results, and discuss how they relate to an emergent view of FAs as mechanosensors. Finally, we will present an outlook to future work in this exciting field.

2. Experimental method

The fabrication of micro-patterned elastic substrates is shown schematically in Fig. 1. A pattern of photoresist (Microposit S1805, Shipley) was produced on Si wafers using standard optical lithography. PDMS elastomer (Syl-

gard 184, Dow Corning) was poured onto glass coverslips, partially cured, put in contact with the photoresist pattern, and cured again. After peeling off, the PDMS film features a topographic modulation, which can be detected easily in phase-contrast microscopy. Alternatively, a fluorescence pattern can be created by using GaAs wafers, because in this case, the fluorescent photoresist remains in the polymer gel during peeling. Typically, a $2 \mu\text{m}$ square lattice of $0.5 \mu\text{m}$ diameter dots with depth $0.3 \mu\text{m}$ was created on a $40\text{-}\mu\text{m}$ -thick film. Varying the ratio of silicone elastomer to curing agent from 10:1 to 50:1 resulted in a Young modulus varying from 1000 to 12 kPa (the Poisson ratio was always close to 0.5). The elastic substrates were coated with fibronectin and cells (human foreskin fibroblasts, cardiac fibroblasts and cardiac myocytes) transfected with GFP-vinculin were plated onto them. Observations were made for mature adhesion, 10–60 h after plating. Image acquisition, image processing and data analysis were performed with DeltaVision, Priism and Matlab software, respectively. Identifying the dot centers in the phase-contrast pictures of substrates deformed by cell traction relatively to the undeformed substrates resulted in deformation data. Fluorescence pictures were processed by identifying clusters of

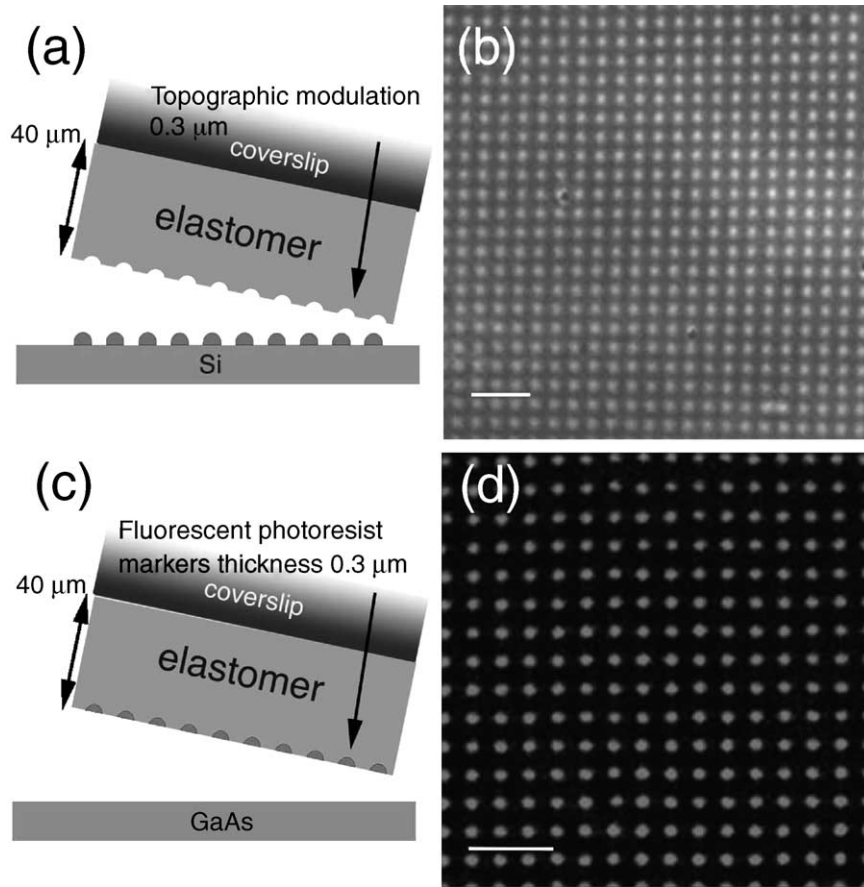


Fig. 1. Fabrication of micro-patterned elastic substrates. (a) Peeling off the elastomer from the Si mould results in a topographic modulation. (b) Phase-contrast image of such pattern. (c) Peeling off the elastomer from the GaAs mould results in the embedding of the photoresist in the elastomer. (d) Fluorescence image of such pattern. Bar = $6 \mu\text{m}$. Reprinted by permission from Ref. [29].

GFP-vinculin. Using the water algorithm [31], an ellipse was fitted to each cluster. This resulted in data on position, size and elongation of FAs (identified with midpoint, area and long axis of the ellipses). For more details on the experimental method, see Ref. [29].

3. Computational method

Since the adhering cells are rather flat, forces exerted onto the substrate can be considered to be tangential to the plane of the substrate surface. Since surface displacements are much smaller than film thickness, one can use linear elasticity theory for an elastic isotropic halfspace. For incompressible elastic substrates (Poisson ratio equals 0.5), the resulting displacement of the substrate surface remains within the plane of the substrate surface [20]. Therefore, the whole elastic problem becomes two-dimensional. Since we never observed displacements in areas deprived of FAs, we assumed that forces are exerted mainly at the sites of FAs. For a collection of discrete forces F at positions r' , the displacement field u at position r is:

$$u(r) = \sum_{r'} G(r - r') F(r')$$

where G is the Green function of the elastic isotropic halfspace, that is, a tensor of rank two:

$$G_{ij}(r) = \frac{3}{4\pi E r} \left(\delta_{ij} + \frac{r_i r_j}{r^2} \right)$$

Here, δ_{ij} denotes Kronecker Delta and E Young modulus. The Poisson ratio has been set to 0.5. The indices i, j take the values 1, 2. For a discrete set of displacement data, the relationship between forces and displacement is a discretized Fredholm integral equation of the first kind. Since these kinds of equations describe smoothing operations that remove high-frequency information, their inversions are ill-posed, that is, the resulting force pattern F will be very sensitive to small changes in the displacement data u . In the presence of experimental noise, ill-posed problems have to be regularized [22,32], that is, one has to estimate the force pattern under a side constraint which in itself is not ill-posed. In our case, a reasonable constraint is that forces should not be exceedingly large. This amounts to zero-order Tikhonov regularization:

$$\min_F \{ |GF - u|^2 + \lambda^2 |F|^2 \}$$

Here, forces and displacements have been written each as one large vector, and G has been redefined correspondingly. Since this target function is quadratic, it can easily be solved by singular value decomposition. The regularization procedure introduces one free variable, the regularization parameter λ . One reasonable criterion for the choice of λ is the discrepancy principle, which states that the residual norm,

$|GF - u|^2$ as a function of λ , should assume the value expected for an optimal fit, $2(N - M)\sigma^2$. Here, N and M are the numbers of discrete displacements and forces, respectively, and σ is the standard deviation of the displacement noise, which we determined experimentally to be in the order of 1 pixel (0.133 μm). Note that although the reconstructed force pattern is an estimate of the original (cellular) one, on the computational side, there is only one unique solution to our procedure. In particular, no energy minimization is required, which might trap the algorithm in some local minimum. For more details on the computational method, see Ref. [30].

4. Results

The combination of experimental setup and computational method described above allowed, for the first time, to measure cellular force at the level of FAs and to correlate it with aggregation characteristics [29]. Fig. 2 shows fluores-

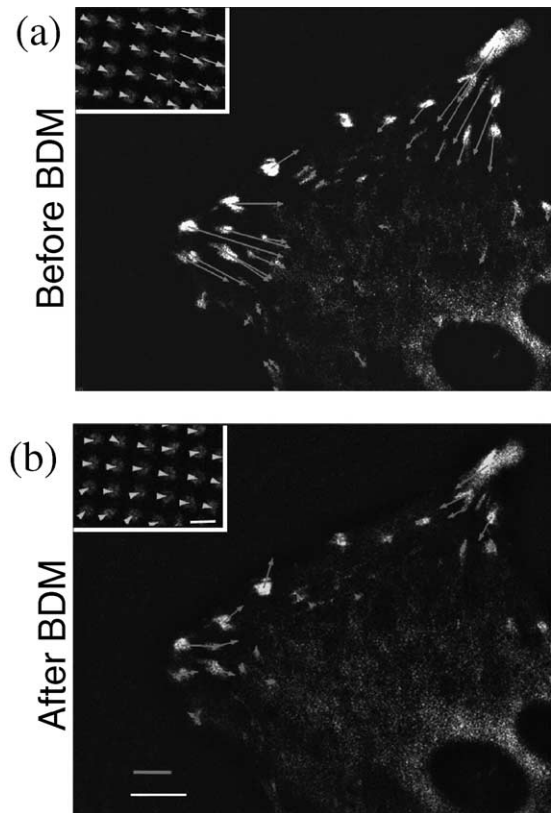


Fig. 2. (a) Fluorescence image of a human foreskin fibroblast expressing GFP-vinculin, which localizes to focal adhesions. Inset: fluorescence image of the pattern of dots below the left-hand side of the cell. Arrows in inset: displacements extracted by image processing. Arrows in main picture: forces calculated from displacements under the assumption that forces are exerted only at focal adhesions as marked by GFP-vinculin. (b) Same as in (a), but 2 min after addition of BDM, which interferes with actomyosin contractility. Both forces and sizes of focal adhesions have diminished. Space bar = 4 μm , force bar = 10 nN, Young modulus = 12 kPa. Reprinted by permission from Ref. [29].

cence images of human foreskin fibroblasts expressing GFP-vinculin. Accumulation of vinculin indicates focal adhesions, which are identified by image processing. On the midpoint of each focal adhesion, we plot the corresponding force vector calculated from the displacement data (displacement vectors are shown in the insets). Typical forces at mature FAs of human foreskin and cardiac fibroblasts were found to vary between 10 and 30 nN. For cardiac myocytes, FAs are larger (albeit somehow less well defined), with forces up to 70 nN. Since each cell can have several hundred FAs, the overall force exerted by a single cell goes up to the μN range. Our main result was that force correlates strongly with aggregation at FAs, as shown in Fig. 3. First, we found a linear relationship between magnitude of force and FA area. Second, direction of force usually agreed with FA elongation. Third, this linear relationship persisted even during the process of FA disruption after addition of 2,3-butanedione monoxime (BDM), which interferes with actomyosin contraction (in Fig. 2, the left and right images are taken before and 2 min after addition of BDM, respectively). In detail, we found that there exists a force-independent size of FAs of the order of $1 \mu\text{m}^2$. For larger areas, force grows in proportion with area, with a

stress constant of $5.5 \text{ nN}/\mu\text{m}^2$. The relationship between area A and force F can thus be written as $A = 1 \mu\text{m}^2 + F \cdot 0.2 \text{ nN}/\mu\text{m}^2$. Addition of BDM leads to simultaneous relaxation of FA force and disruption of FA aggregation on a time scale of seconds. Surprisingly, we found that the linear relation between force and area persists even in the process of FA disassembly, indicating that a fast process provides some kind of equilibration on a time scale faster than the time scale of FA disassembly.

The resolution of elastic substrate experiments is difficult to access since it depends on the details of the force pattern applied. We have used data simulation to estimate the resolution of our method [30]. An example from this analysis is shown in Fig. 4. By choosing force patterns F_0 resembling cellular traction patterns, we were able to monitor the quality of force reconstruction as a function of all parameters involved (area density, magnitude and direction of cellular forces, area density of displacement data, substrate elastic constants, and noise level). We found that even under the most favourable conditions which we had achieved experimentally, the original force could not be reproduced completely (typical deviation $\Delta F = |F - F_0| / |F_0| > 20\%$, where F is force reconstructed with regulariza-

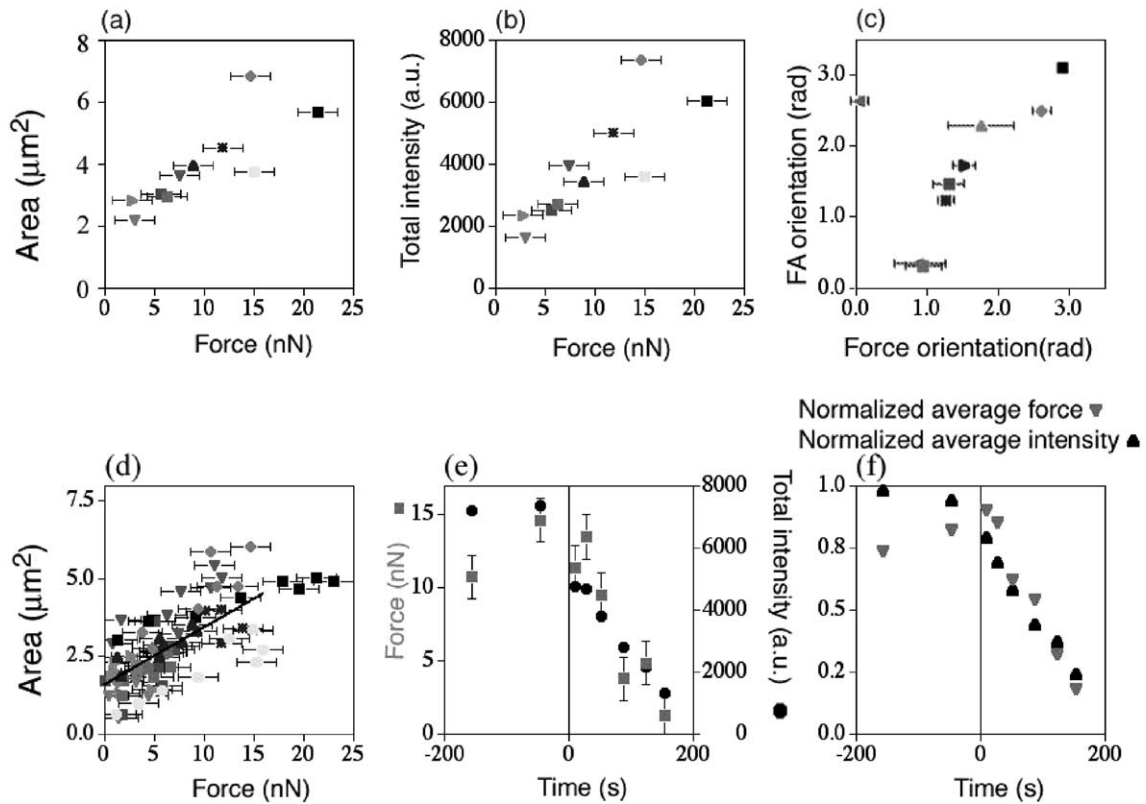


Fig. 3. Correlation between force and aggregation at focal adhesions. (a, b, c) Before addition of BDM, data from Fig. 2a. (d, e, f) After addition of BDM, data from Fig. 2b. (a) Correlation between force and area of single focal adhesions. (b) Correlation between force and total fluorescence intensity of single focal adhesions. (c) Correlation between the directions of forces and the elongations of the focal adhesions. (d) Like in (a), but for all time points. The black line defines a stress constant of $5.5 \text{ nN}/\mu\text{m}^2$. (e) Relaxation of force (squares) and total fluorescence intensity (dots) for one single focal adhesion as a function of time. (f) Relaxation of force (triangles pointing down) and total fluorescence intensity (triangles pointing up) averaged over all focal adhesions. Reprinted by permission from Ref. [29].

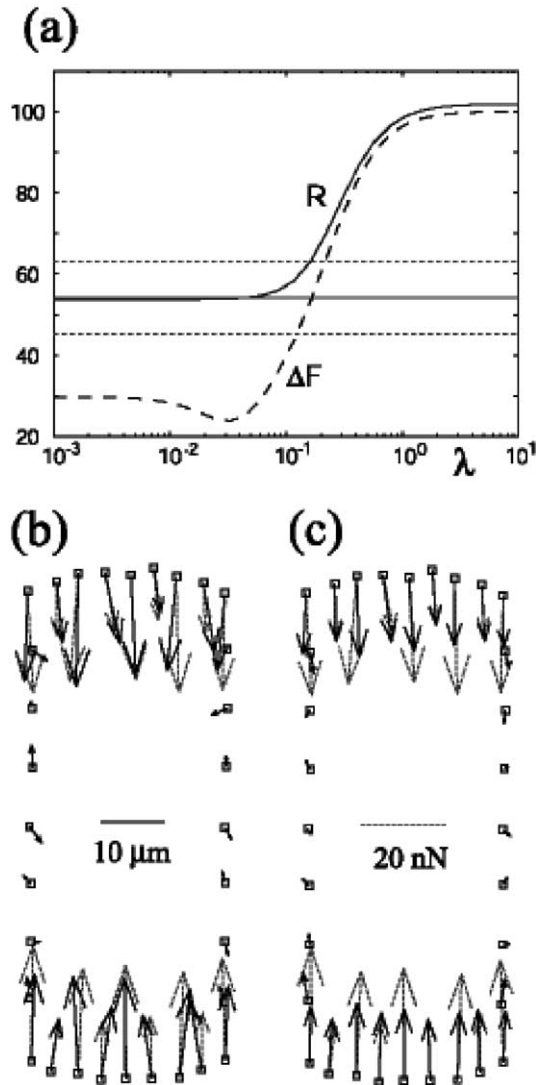


Fig. 4. Data simulation is used to estimate resolution: for an artificial force pattern F_0 , theoretical displacement u is calculated. After addition of noise, a force pattern F is reconstructed and compared with the initial one. (a) Residual norm $R = |GF - u|^2$ (absolute values) and deviation from original force $\Delta F = |F - F_0|/|F_0|$ (in percent) as a function of regularization parameter λ . Straight lines indicate the confidence interval for the corresponding χ^2 -estimate. For optimal regularization ($\lambda = 0.04$), ΔF attains a minimum and R the χ^2 -expectation value. Note that even in this case, 24% of the original force has been lost in the reconstruction; without regularization ($\lambda = 0$), 30% is lost. (b) Original (dashed) and reconstructed (solid) forces for $\lambda = 0.04$. Spatial and force reconstructions are around $4 \mu\text{m}$ and 4 nN , respectively. (c) The same for $\lambda = 0.1$. Both spatial and force resolution have worsened considerably. Reprinted by permission from Ref. [30].

tion). This indicates that in the presence of noise, information is irreversibly lost during the smoothing process of converting forces into displacements. We also found that regularization is required to arrive at a reliable estimate (otherwise ΔF becomes considerably larger, $\Delta F > 30\%$). In less favourable cases, ΔF can become larger than 40% and 60% in the cases of optimal and missing regularization, respectively. Although it is difficult to make general state-

ments about resolution, we found that in realistic cases, spatial and force resolution are better than $4 \mu\text{m}$ and 4 nN , respectively. One direct consequence of the limited spatial resolution is that only those FAs have been used in our correlation analysis, which are correspondingly well separated from other FAs. Using the concept of a force multipolar expansion, one can show that the assumption of localized force is reasonable as long as displacements are picked up at a distance to the FAs which is larger than their lateral dimensions. The same concept can also be used to show that the assumption of an elastic halfspace is reasonable as long as the displacements are smaller than film thickness.

5. Discussion

Force at fibroblast FAs was found to have a typical value of 20 nN , which is consistent with results both from other experiments with mechanically active cells [26,33], and from single molecule experiments [34,35]. The energy scale of single molecules is determined by ATP hydrolysis, that is, by thermal energy kT . With Boltzmann constant k and room temperature T , one has $kT = 4.14 \text{ pN nm}$, thus, conformational changes in the nm-range correspond to forces in the pN-range (e.g. the stall force for kinesin is 5.5 pN [34], and the static rupture force for biotin–avidin is 5 pN [35]). Since several thousands of integrin adhesion molecules and of myosin II molecular motors correspond to one FA, the pN-scale of single molecules is amplified to the nN-range at FAs.

FAs feature different morphologies, compositions and force magnitudes depending on the cellular state. In their early work with elastic substrates, Harris et al. [15,16] found that cells exert much stronger forces than needed for locomotion (viscous dissipation of cell-sized objects leads to miniscule forces in the fN-range). They concluded that cells might use strong forces for matrix remodelling during development and tissue maintenance. An additional aspect of forces at FAs has become clear during recent years: FAs seem to act as mechanosensors, that is, forces are used to actively probe the mechanical properties of the environment [2–4]. In particular, it has been shown that forces applied at FAs are converted into biochemical signals that trigger signalling pathways [8,9]. Our study clearly shows that the mechanosensory function of FAs is coupled to their aggregation behaviour. There are different possibilities for the detailed functioning of this mechanosensor, including large-scale reorganization of FAs under force and force-induced opening of specific molecules.

The spatial resolution of the force field is inherently restricted by the smoothing action of elasticity theory. Smoothing takes place on the length scale $(F/E)^{1/2} = \mu\text{m}$ set by cellular forces $F = \text{nN}$ and substrate rigidity $E = \text{kPa}$. This implies that softer substrates worsen resolution (they also might result in changes in cell behaviour). Since stiffer substrates do not yield large enough displacements, we can

conclude that there is only a certain window for reasonable substrate stiffness in elastic substrate experiments. Nevertheless, there are few alternatives to elastic substrate work. One promising route seems to be the use of local strain gauges like cantilevers etched into silicon wafers [33]. Methods like this avoid the inherent limitation of elastic bulk material discussed above.

It is intriguing to note that in many cases, cells show a pinching force pattern [24,26,30,36]. There are several reasons to explain this observation. First, cells are usually in mechanical equilibrium (this essentially holds for cell locomotion as well, since here, unbalanced forces might appear only during relatively short times of back retraction). Then, Newton's third law predicts that the overall force has to vanish. The simplest way to achieve this is by the pinching pattern. Second, the build-up of stress fibres results from a positive feedback mechanism, which once started for a certain direction, might quickly suppress build-up of stress fibres in competing directions. Third, cells in physiological situations often adhere to one single fibre, which then enforces the pinching force pattern. Using data from our study (not shown), we can conclude that in the framework of a force multipolar expansion, many mechanically active cells can be modelled as anisotropic force contraction dipoles with a strength of 10^{-11} J (this corresponds to a pair of forces, each 200 nN strong and separated by 60 μ m). Although at this stage, the concept of a force dipole is a theoretical model which still has to prove its capability to predict experimental observations of cellular organization in elastic media, it appears to provide an interesting framework for future modelling, for example, large-scale assembly of elastically interacting cells in a soft medium [37].

6. Outlook

On the side of *molecular cell biology*, an intriguing aspect for future work in this field is the mechanosensory mechanism of FAs. This problem might be best approached by single molecule experiments. At the same time, attention will probably shift to situations that are closer to physiological situations like softer substrates and three-dimensional gels. We expect that in the future, fluorescence microscopy will be used to simultaneously monitor as many different components of FAs as possible.

On the side of *materials sciences*, the use of micro-patterned substrates opens up completely new possibilities to achieve more insight and better control of cellular behaviour. In the future, surfaces might be structured regarding their topographical, elastic and chemical properties. Potential applications include manipulation of single cells (e.g. on biochips and biosensors), as well as manipulation of large cell communities (e.g. for tissue engineering). For example, it might become feasible that cells are positioned and induced to fuse in a well-controlled environment in order to design artificial tissues or organs.

On the side of *theoretical modelling*, there is a strong need for both fast and reliable algorithms to quantitatively evaluate experiments and for theoretical understanding of aggregation and signalling behaviour at FAs. For example, it might be well that mechanosensing at FAs is based on statistical properties of molecular interactions in FAs in the presence of force. Given the importance of mechanosensing for many different cell types like fibroblasts, endothelial cells, leukocytes, muscle cells and neurons, any advance in this field would be highly welcome.

References

- [1] B. Alberts, A. Johnson, J. Lewis, M. Raff, K. Roberts, P. Walter, *Molecular Biology of the Cell*, Garland Science, New York, 2002.
- [2] C.G. Galbraith, M. Sheetz, *Curr. Opin. Cell Biol.* 10 (1998) 566.
- [3] M.E. Chicurel, C.S. Chen, D.E. Ingber, *Curr. Opin. Cell Biol.* 10 (1998) 232.
- [4] S. Huang, D.E. Ingber, *Nat. Cell Biol.* 1 (1999) E131.
- [5] T. Korff, H.G. Augustin, *J. Cell Sci.* 112 (1999) 3249.
- [6] G.F. Oster, J.D. Murray, A.K. Harris, *J. Embryol. Exp. Morphol.* 78 (1983) 83.
- [7] R.T. Tranquillo, *Biochem. Soc. Symp.* 65 (1999) 27.
- [8] D. Choquet, D.F. Felsenfeld, M.P. Sheetz, *Cell* 88 (1997) 39.
- [9] D. Riveline, E. Zamir, N.Q. Balaban, U.S. Schwarz, B. Geiger, Z. Kam, A.D. Bershadsky, *J. Cell Biol.* 153 (2001) 1175.
- [10] B. Geiger, A. Bershadsky, R. Pankov, K.M. Yamada, *Nat. Rev. Mol. Cell Biol.* 2 (2001) 793.
- [11] C.K. Miranti, J.S. Brugge, *Nat. Cell Biol.* 4 (2002) 83.
- [12] M. Abercrombie, G.A. Dunn, *Exp. Cell Res.* 92 (1975) 57.
- [13] W. Chen, S.J. Singer, *J. Cell Biol.* 95 (1982) 205.
- [14] E. Cukierman, R. Pankov, D.R. Stevens, K.M. Yamada, *Science* 294 (2002) 1708.
- [15] A.K. Harris, P. Wild, D. Stopak, *Science* 208 (1980) 177.
- [16] A.K. Harris, D. Stopak, P. Wild, *Nature* 290 (1981) 249.
- [17] K.A. Beningo, Y.-L. Wang, *Trends Cell Biol.* 12 (2002) 79.
- [18] P. Roy, Z. Rajfur, P. Pomorski, K. Jacobson, *Nat. Cell Biol.* 4 (2002) E91.
- [19] K. Burton, D.L. Taylor, *Nature* 385 (1997) 450.
- [20] L.D. Landau, E.M. Lifshitz, *Theory of Elasticity*, Pergamon, Oxford, 1970.
- [21] J. Lee, M. Leonard, T. Oliver, A. Ishihara, K. Jacobson, *J. Cell Biol.* 127 (1994) 1957.
- [22] W.H. Press, S.A. Teukolsky, W.T. Vetterling, B.P. Flannery, *Numerical recipes in FORTRAN, The Art of Scientific Computing*, Cambridge Univ. Press, Cambridge, 1992.
- [23] M. Dembo, T. Oliver, A. Ishihara, K. Jacobson, *Biophys. J.* 70 (1996) 2008.
- [24] T. Oliver, M. Dembo, K. Jacobson, *J. Cell Biol.* 145 (1999) 589.
- [25] R.J. Pelham, Y.-L. Wang, *Proc. Natl. Acad. Sci. U. S. A.* 94 (1997) 13661.
- [26] M. Dembo, Y.-L. Wang, *Biophys. J.* 76 (1999) 2307.
- [27] C.-M. Lo, H.-B. Wang, M. Dembo, Y.-L. Wang, *Biophys. J.* 79 (2000) 144.
- [28] K.A. Beningo, M. Dembo, I. Kaverina, J.V. Small, Y.-L. Wang, *J. Cell Biol.* 153 (2001) 881.
- [29] N.Q. Balaban, U.S. Schwarz, D. Riveline, P. Goichberg, G. Tzur, I. Sabanay, D. Mahalu, S. Safran, A. Bershadsky, L. Addadi, B. Geiger, *Nat. Cell Biol.* 3 (2001) 466.
- [30] U.S. Schwarz, N.Q. Balaban, D. Riveline, A. Bershadsky, B. Geiger, S.A. Safran, *Biophys. J.* 83 (2002) 1380.
- [31] E. Zamir, B.-Z. Katz, S. Aota, K.M. Yamada, B. Geiger, Z. Kam, *J. Cell Sci.* 112 (1999) 1655.

- [32] P.C. Hansen, Rank-deficient and Discrete Ill-posed Problems, SIAM, Philadelphia, PA, 1998.
- [33] C.G. Galbraith, M.P. Sheetz, Proc. Natl. Acad. Sci. U. S. A. 94 (1997) 9114.
- [34] K. Visscher, M.J. Schnitzer, S.M. Bloch, Nature 400 (1999) 184.
- [35] R. Merkel, P. Nassoy, A. Leung, K. Ritchie, E. Evans, Nature 397 (1999) 50.
- [36] J.P. Butler, I.M. Tolic-Norrelykke, B. Fabry, J.J. Fredberg, Am. J. Physiol., Cell Physiol. 282 (2002) C595.
- [37] U.S. Schwarz, S.A. Safran, Phys. Rev. Lett. 88 (2002) 048102.